Journal Pre-proofs

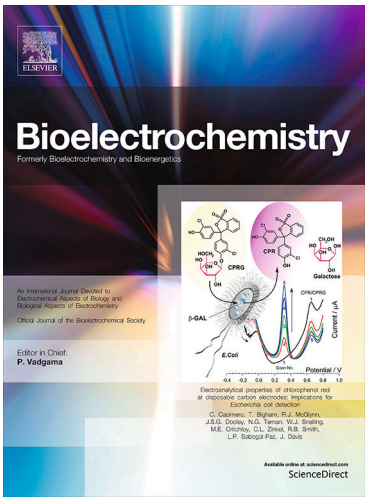

Construction of manganese oxide nanowire-like cluster arrays on a DNA template: application to detection of hydrogen peroxide

Nader Amini, Mojtaba Shamsipur, Afshin Maleki

PII: S1567-5394(19)30252-X
DOI: https://doi.org/10.1016/j.bioelechem.2019.107419
Reference: BIOJEC 107419

To appear in: *Bioelectrochemistry*

Received Date: 20 April 2019
Revised Date: 14 November 2019
Accepted Date: 17 November 2019

Please cite this article as: N. Amini, M. Shamsipur, A. Maleki, Construction of manganese oxide nanowire-like cluster arrays on a DNA template: application to detection of hydrogen peroxide, *Bioelectrochemistry* (2019), doi: https://doi.org/10.1016/j.bioelechem.2019.107419

Construction of manganese oxide nanowire-like cluster arrays on a DNA template: application to detection of hydrogen peroxide

[a]Nader Amini□, [b]Mojtaba Shamsipur □□, [a]Afshin Maleki

[a]*Environmental Health Research Center, Research Institute for Health Development, Kurdistan University of Medical Sciences, Sanandaj, Iran*

[b]*Department of Analytical Chemistry, Razi University, Kermanshah, Iran*

Abstract

Improved electron transfer properties and catalytic activity of manganese oxide (MnOx) was demonstrated following its electrochemical deposition on a deoxyribonucleic acid (DNA) modified glassy carbon electrode. The MnOx showed different morphologies, electrocatalytic properties and electrochemical kinetics. Scanning electron microscopy showed that electrodeposition of MnOx on a bare glassy carbon electrode led to the formation of irregular-shapes while a nanowire cluster (NWC) was formed on a GCE/DNA due to the DNA serving as a template. Electrochemical impedance spectroscopy (EIS) revealed lower charge transfer resistance of the MnOxNWC compared with MnOx. A new mechanism is presented for the electrodeposition of MnOx on the surface of a GC/DNA electrode. An electrochemical biosensor was fabricated based on depositing MnOx onto a glassy carbon /DNA electrode (GCE/DNA/MnOxNWC) and was used to detect hydrogen peroxide (H_2O_2). The MnOx nanowire cluster and DNA exhibited significant electrocatalytic activity for simultaneous electrocatalytic oxidation at two oxidation potentials (0.6V and 0.98V vs Ag/AgCl) and one reduction potential (-0.5V vs Ag/AgCl) for H_2O_2 at pH 6.0. A new mechanism for the detection of H_2O_2 is presented. Excellent electrocatalytic activity, stability and facility for simultaneous detection of H_2O_2 at different of applied potentials are proposed advantages of the proposed electrochemical biosensor.

Keywords: DNA template; MnOx nanowire cluster; Hydrogen peroxide, Simultaneously

---

*Corresponding author:Tel: +98 9183761209,Email address: mshamsipur@yahoo.com naderamini95@yahoo.com

1. Introduction

For various applications, the size and shape of nanomaterials play an important role [1]. The fabrication of novel nanoparticles-biomolecule hybrid systems by biomaterials assembled on suitable surfaces is of considerable interest. Biomolecules can provide templates for the immobilization of nanoparticles [2]. Deoxyribonucleic acid (DNA) is an essential biomolecule with a chain length of 2 μm and a diameter of 2 nm, and this organisation can lead to the formation of various nanostructures. DNA is a potential template for fabricating some specified materials and creating nanoassemblies; selective base-pairing interactions between complementary single-strand DNA chains are reported to have been applied [1,3]. Moreover, native double helical deoxyribonucleic acid is an appropriate option for interacting directly with metal ions and their complexes. As a result, DNA is a good template for fabricating one-dimensional nanoparticles. Thus far, the presence of various metals on DNA have been reported, but the immobilization of metal nanoparticles remains a challenge [3-4]. The deposition of NiO [5], Ag [6], Au [7], Pt [8] and Pd [9] on DNA has been reported as a potential approach for the preparation of nanoshapes and nanowires. The measurement of hydrogen peroxide (H_2O_2) has become important because it has many applications. Thus, H_2O_2 (HP) is used as a fundamental species in the pharmaceutical, clinical, food and environmental sectors and it is produced by a great number of enzymes [10]. The development of reliable, sensitive and accurate methods for H_2O_2 detection is assuming practical importance. Thus far, many techniques such as titration [12], spectrophotometry [13], fluorometry [14], chemiluminescence [15] and chromatography [16] have been proposed for the determination of hydrogen peroxide [11]. Although reports provide clear benefits for its the detection, they are costly, complex and potentially polluting for the environment. In general, in electrochemical analysis, the electroreduction or electrooxidation of H_2O_2 is not feasible at the surface of a bare glassy carbon electrode. Such electrodes manifest high-over potentials and slow electron transfer for either oxidation or reduction of H_2O_2. To overcome this challenge, modified electrodes are used [17].

Many modifiers have been used to fabricate electrochemical sensors such as enzymes [18], protein molecules [19], complexes of transition metals [20], dye materials [21] and nanomaterials [22] for the detection of hydrogen peroxide. Manganese oxide (MnOx) is a type of attractive metal oxide material and shows catalytic activity towards hydrogen peroxide. Various types of MnOx nanomaterials have been used in the construction of

electrochemical sensors based on hydrogen peroxide catalytic activity [23-24]. Manganese oxides can be formed using various techniques such as coprecipitation [25], simple chemical reduction reaction [26], sol-gel processes [27] and thermal decomposition [28]. Nevertheless, it is to some extent difficult to form the MnOx and the commonly employed nanoparticles on the surface of electrodes because employing the traditional slurry coating technique for nanoparticles have poor dispersibility in the coatings. Thus, electrochemical deposition [29] is considered a powerful alternative for the preparation of metal oxide nanoparticle modified electrodes at room temperature. Various templates have been proposed for the electrodepositation of MnOx. For instance, Wu et al [30] used the electrodeposition method to prepare needle-like manganese oxides onto the surface of a graphite disc electrode. The Shinomiya group [31] reported nano-sized manganese oxide on stainless steel while Pang et al [27] reported the synthesis of MnOx thin films onto nickel foils. In this paper, an electrochemical technique was utilized for the preparation of a manganese oxide nanowire-like cluster with DNA as template, and for its application in the electrocatalytic reduction and oxidation of H_2O_2 at pH 7. 2.

2. Experimental

2.1. Materials and reagents

Calf thymus (CT) DNA (highly polymerized, sodium salt, type XI, 42% GC content) was prepared from purchased from Sigma-Aldrich and it is used as received without further purification. Buffer solutions (0.1 M) were prepared from di- sodium hydrogen phosphate and sodium dihydrogen phosphate. pH adjustment was performed with hydrogen chloride or sodium hydroxide. Sodium sulfate, hydrogen peroxide, manganese sulphate, potasium chloride, hydroquinone and $K_3[Fe(CN)_6]/K_4[Fe(CN)_6]$ were all purchased from Merck company.

2.2. Apparatus

All the electrochemical experiments were performed with a µ-Autolab modular electrochemical system and GPES software (Eco Chemie U/techt, the Netherlands). A three-electrode system including Pt wire as auxiliary electrode, glassy carbon (GC) as working electrodes and Ag/AgCl [KCl (sat)] as reference electrode was used. For the investigation of the surface morphology of electrodes, a Vega-Tescan electron microscope

was employed. The pH values were checked using a pHs-3C pH meter (Shanghai Analytical Instrument Factory, China).

2.3. General analytical procedure

Electrochemical impedance spectroscopy (EIS) analysis was used in the presence of a 3mM $[Fe(CN)_6]^{3-/4-}$ as a charged probe at a bias potential of 0.6 V vs Ag/AgCl and with 1 mM hydroquinone solution as a neutral probe at 0.8 V vs Ag/AgCl in the frequency range from 0.01 to 10^4 Hz. The electrochemical behavior of the GC/DNA/MnOxNWC electrode was characterized by cyclic voltammetry. Additionally, the electrooxidation and electroreduction properties of the modified electrode were investigated by cyclic voltammetry in the potential range of -1 to +1.5 V vs Ag/AgCl and a step potential of 0.025 V vs Ag/AgCl at pH 7. Amperometric hydrogen peroxide determination on a GC/DNA/MnOxNWC electrode was obtained by addition of successive amounts of sample.

2.4. Electrode preparation and modification

Alumina paste was used for mechanically polishing the bare GCE which was then ultrasonicated for 4 min in ethanol and distilled water to remove adsorbed particles. Then, the electrode was immersed in a 1.0 mg ml^{-1} of DNA solution and the electrode modified by the chronoamperometric method by applying a constant potential of -1.5 V vs Ag/AgCl for 40 min. Next, it was rinsed with distilled water. MnOx was deposited on the surface attached DNA forming nanowire-like cluster structures. Finally, electrocatalytic reduction and oxidation of H_2O_2 was investigated (Schematic 1).

Schematic 1

3. Results and discussion

3.1. Electrodeposition of manganese oxide nanowire clusters

Figure1A displays the CVs for the GC/DNA electrode containing 1mM $MnSO_4.2H_2O$ and 0.1 M Na_2SO_4 at the potential range of − 0.8 to 1.8 V vs Ag/AgCl at a scan rate of 10 mVs^{-1}. Current peaks increased with a subsequent scans, consistent with the progressive formation of manganese oxide nanoparticles indicating that MnOx was deposited on the

surface of the GC electrode (Equations 1 to 9). An anodic peak was observed at +0.8V vs Ag/AgCl (first cycle) which corresponds to the oxidation of Mn2+ in solution to a solid species and this species is then reduced in four steps on the surface of the GC/DNA electrode. According to Petitpierre et al [32], step R1 can be attributed to the reduction of solution species available near the working electrode. Based on previous reports [33-35], the two later steps (R2 and R3) correspond to the electroreduction of Mn (IV) to Mn (II) via intermediate Mn(III) species. Step R4 can be ascribed to the dissolution of manganese (II) hydroxide, with solid Mn (II) converted to soluble Mn(II). During the second scan, the solid species present on the surface of GCE at the end of the cathodic scan is then electro-oxidized back to Mn (IV) in four steps (noted as O4, O3, O2 and O1).The anodic peak O4 might be related to the oxidation of an Mn(II) to a mixed Mn(II)–Mn(III) species, the anodic peak O3 to the oxidation of Mn(II)–Mn(III) to an Mn(III) species, the oxidation peak O2 corresponds to the oxidation of this latter species to an Mn(III)–Mn(IV) mixed compound and the anodic peak O1 attributed to the oxidation of this last species to an Mn(IV). Moreover, the rise in peak intensities with the cycle scan number suggests that manganese compounds employed in this mechanism have low solubility and are suitable for electron transfer [36]. The findings demonstrate that when the CV scan reaches 8 cycles, peak currents scarcely escalate, indicating a cessation of electrodeposition. A new mechanism can be proposed based on some previously published reports [36].

Figure 1

Scan 1

$Mn^{3+} + e^- \rightarrow Mn^{2+}$ (R1) (1)

$MnO_2 + H^+ + e^- \rightarrow MnOOH$ (R2) (2)

$MnOOH + H^+ + e^- \rightarrow Mn(OH)_2$ (R3) (3)

$Mn(OH)_2 + 2H^+ + 2e^- \rightarrow Mn(s) + 2H_2O$ (R4) (4)

Scan 2

$3Mn(OH)_2 \rightarrow Mn_3O_6 + 2H_2O + 2H^+ + 2e^-$ (5)

And (O4)

$Mn(s) \rightarrow Mn^{2+} + 2e^-$ (6)

$Mn_3O_4 + 2H_2O \rightarrow 3MnOOH + H^+ + e^-$ (O3) (7)

$7MnOOH \rightarrow Mn_7O_{13} + H_2O + 5H^+ + 5e^-$ (O2) (8)

$Mn_7O_{13} + H_2O \rightarrow 7MnO_2 + 2H^+ + 2e^-$ (O1) (9)

3.2. Morphology characterization of modified electrodes

By scanning electron microscopy, the surface morphology of different electrodes (GC/MnOx and GC/DNA/MnOxNWC) were investigated. The SEM images showed that the MnOx electrodeposited on the surface GCE are different in their shape and size from those of glassy carbon modifided with DNA. Figure 1B (a) displays the morphology of GCE/MnOx where nanostructured irregular-shaped nanoparticles agglomerated to micron size morphology for MnOx. SEM images of the GC/DNA/MnOxNWC electrode indicates the creation of regular-shape structures with an average diameter of 100 nm and nanowire-like clusters (Figure1B (b and c)). When DNA is used on the surface of the GC electrode as templates, the assemblies of nanoparticles obtained might have an organisation dependent on the model produced on the DNA immobilization.

3.3. Electrochemical characterization: voltammetric study

The electrochemical activity of the electrodeposited DNA/MnOxNWC was studied by recording cycling voltammograms of the modified electrodes in 1mM hydroquinone. Cyclic voltammograms were recorded at bare GC, GC/DNA, GC/MnOx and GC/DNA/MnOxNWC electrodes. The results are presented in Figure 2A. As can be seen in curve a, a pair of well-defined redox peaks can be obtained at an unmodified GC electrode with $\Delta Ep = 610$ mV. Curve c shows that the assembly of DNA on GCE led to an increase in the peak separation ($\Delta Ep = 690$ mV) of the redox probe due to the

insulating behavior of DNA. After the bare electrode was modified with MnOx, a large increase in the current and a decrease in ΔEp were observed (curve b). The current response at the GC/DNA/MnOxNWC electrode increased greatly compared with that at the GC/MnOx electrode which can be attributed to the high conductivity of MnOxNWC and a greater ease of electron transfer on to the DNA template (curve d).

Figure 2

Figure 2 The effective surface area was investigated by cyclic voltammetry in 3mM $[Fe(CN)_6]^{3-/4-}$ and 0.1 M KNO_3 probe at different scan rates (10 -100 mVs^{-1}) using the Randles–Sevcik equation (Eq 10).

$$I_p = (2.69 \times 10^5)\, n^{3/2} D^{1/2}\, CAv^{1/2} \qquad \text{(Eq 10)}$$

Where n is the number of transferred electrons, D is the diffusion coefficient ($6.70 \times 10^{-6} cm^2\ s^{-1}$), C is the concentration of probe (3 mM), A is the effective surface area (cm^2), and v is the scan rate ($V\ s^{-1}$). For cycling voltammetry using $[Fe(CN)_6]^{3-/4-}$ with n=1, the amount of A values was calculated to be 0.032 cm^2 and 0.038 cm2 for GC/MnOx and GC/D NA/MnOxNWC electrodes, respectively [37]. This behavior could be an outcome of the immobilization of DNA and might produce a template on the surface of electrode increasing the surface area of the GCE.

3.4. Electrochemical impedance spectroscopy study by the charged probe

Electrochemical impedance spectroscopy (EIS) is an interesting method for studying the electrochemical outcome of the modification process at an electrode using an electroactive species, charged probe such as the $[Fe(CN)_6]^{3-/4-}$ couple. Figure 2C (a-d) compares the cyclic voltammetric responses obtained at the bare glassy carbon (curve a), GC/MnOx (curve b), GC/DNA (curve c) and GC/DNA/MnOxNWC (curve d) electrodes for the $[Fe(CN)6]^{3-/4-}$ probe. The results indicate that at a 100 mV s^{-1} scan rate in 0.1 M KCl, the ferricyanide couple presents reversible behavior at a plain GC electrode and ΔEp is approximately 80 mV. For the GC/DNA electrode, the peak currents were very low and demonstrated a reversible response. Higher peak currents were observed at the GC/DNA/ MnOxNWC electrode when compared with the other electrodes. Figure 2D(a-d)

illustrates the impedance spectra indicated as Nyquist plots (Zim vs. Zre) for different electrodes such as bare GC (a), GC/MnOx (b), GC/DNA (c) and GC/DNA/ MnOxNWC (d) electrodes in the frequency range of 0.01–10^4 Hz, at 0.6 V vs Ag/AgCl and in 3mM $[Fe(CN)_6]^{3-/4-}$ as an electrochemical probe. As observed from the Nyquist plots 2D (a-d), the Rct value for the GC/DNA electrode (curve c) shows a significant increase compared to the GC bare electrode (curve a). The observed behavior might be related to repulsion force between negatively charged DNA on the surface of electrode and the ferricyanide ion. The EIS data were obtained for GC/MnOx (b) and GC/DNA/MnOxNWC electrodes (d). For GC/MnOx electrode (Rct= 0.8 KΩ), a higher figure was obtained than that for the GC/DNA/MnOxNWC electrode (Rct= 0.1 KΩ) under the same conditions. These findings suggest that MnOx promotes electron transfer and indicate a faster electron transfer at the GC/DNA/ MnOxNWC interface compared to that at the GC/MnOx electrode. The decrease of MnOx Rct after immobilization onto GC/DNA electrode compared to the bare glassy carbon electrode might be attributed to i) their different surface morphologies or ii) an electrostatic attraction between the DNA/MnOxNWC surface (positively charged) and the $[Fe(CN)_6]^{3-/4-}$ probe (negatively charged) [5]. To discover the origin of the decrease, EIS was carried out in the presence of hydroquinone as a neutral probe.

3.4.1. Electrochemical impedance spectroscopy study by the neutral probe

Figure 2B(a-d) indicates the impedance spectra represented as Nyquist plots for bare GC (a), GC/MnOx (b), GC/DNA (c) and GC/DNA/MnOxNWC (d) electrodes with 1 mM hydroquinone solution and in the frequency range of 0.01 to 104 Hz and at 0.8 V vs Ag/AgCl as an electrochemical probe. The estimates obtained for the Rct calculated by fitting the data were 326, 116, 137, and 19.1 KΩ for GC, GC/MnOx, GCE/DNA and GC/DNA/MnOxNWC electrodes, respectively. The findings (Section 3.4) are consistent with the EIS experiments using the $[Fe(CN)_6]^{3-/4-}$ probe. Therefore, the assumption of an electrostatic attraction between surface and probe can be discounted. Consequently, DNA can be considered to act as a template for the preparation of nanowire-like cluster with improved charge transfer, producing more sites for the immobilization of MnOx.

3.5. Simultaneous electrocatalytic oxidation and reduction of hydrogen peroxide on GC/ DNA/ MnOxNWC electrode

For the investigation of electrooxidation and electroreduction of hydrogen peroxide at the surface of different electrodes, CV in the presence and absence of H_2O_2 was used. Figure1C shows the CV at modified and unmodified electrodes in the presence and absence of 2000 µM H_2O_2 in 0.1 M buffer solution at pH 7. At the bare GCE (curve a), no observable redox peak in the presence of H_2O_2 was detected, which indicates that the electrooxidation and electroreduction of H_2O_2 requires a large overpotential. Curve b illustrates GC/DNA/MnOxNWC electrode behaviour in the absence of H_2O_2 in a buffer solution at pH 7. As observed, two well-defined anodic peaks (Ox2 and Ox1) and one cathodic peak (Red) appear at +0.6, +0.98 and -0.5V vs Ag/AgCl respectively. For the GC/MnOx electrode in the presence of H2O2 (curve c), two oxidation peaks increased simultaneously and for GC/DNA/MnOxNWC electrode and in the presence of hydrogen peroxide, oxidation peak currents and cathodic peak increased dramatically, which might be due to the electrocatalytic activity of MnOxNWC (curve d). The effect of pH on the electro-chemical behavior of the GC/DNA/MnOxNWC electrode was investigated in the pH range 2-8 and CVs showed a dependence on pH. In acidic buffer (pH 2-3), the diffusion of ions into the MnOx structure makes it unstable and MnO_2 changes to MnOOH which indicates that acidic pHs will lead to performance instability. Furthermore, DNA might be unstable in very acidic and basic media causing oxidation and reduction peaks to be substantially reduced [36]. In order to obtain the optimal pH for the electrooxidation and electroreduction of H_2O_2, the behavior of the GC/DNA/MnOxNWC electrode in the pH range 6 to 8 was investigated in 500 µM hydrogen peroxide by CV. From these results, the maximum response of the proposed electrode (GC/DNA/MnOxNWC) was at pH= 7 and this was selected for subsequent use. The effect of the potential scan rate was also studied in presence of 500 µM H_2O_2 at pH7 (Figure 3A). The plots of the cathodic and anodic peak currents vs the square root of the scan rate (Figure 3B(a-c)) are linear showing that the process is diffusion controlled as expected for a catalytic system.

Figure 3

The behavior of the GC/DNA/MnOxNWC electrode in H_2O_2 samples at various concentrations was investigated (Figure 4A). The modified electrode has good sensitivity and a suitable response towards H_2O_2 in three simultaneous steps: two anodic peaks (Ox1 and Ox2) and one cathodic peak (Red) appeared at +0.6, +0.98 and -0.5V vs Ag/AgCl, respectively. According to previous reports [36,23,38], a possible electrocatalytic mechanism between MnOx and H_2O_2 can be proposed as follows:

OX2:

$$7MnOOH \rightarrow Mn_7O_{13} + H_2O + 5H^+ + 5e^- \quad (11)$$

$$Mn_7O_{13} + 8H_2O_2 \rightarrow 7MnOOH + 7O2 + H_2O \quad (12)$$

OX1:

$$Mn_7O_{13} + H_2O \rightarrow 7MnO_2 + 2H^+ + 2e^- \quad (13)$$

$$2MnO_2 + H_2O_2 \rightarrow Mn_2O_3 + O2 + H_2O \quad (14)$$

Red:

$$MnOOH + H^+ + e^- \rightarrow Mn(OH)_2 \quad (15)$$

$$2Mn(OH)_2 + H^+ + e^- + H_2O_2 \rightarrow MnOOH + 2\,H_2O \quad (16)$$

For the oxidation waves (Ox2 and Ox1): the anodic peak currents which appeared at 0.6 V and 0.98V vs Ag/AgCl increase linearly with H_2O_2 concentration. As observed from Figure 4B(a-c), the linear ranges for Ox2 and Ox1 are 100 to 4200 µM and 200 to 3000 µM with an excellent linear correlation of (R^2 = 0.987) and (R^2 = 0.992), respectively. In addition, the reduction peak of H_2O_2 is proportional to its concentration over the range 100 to 2800 µM (R^2 = 0.993).

Figure 4

3.6. Amperometric detection of hydrogen peroxide at GC/DNA/MnOxNWC electrode

An amperometric method was used to reduce the detection limit and increase sensitivity. Figure 5 shows the standard hydrodynamic amperograms of a rotating (2000 rpm) GC/DNA/MnOxNWC electrode with sequential injection of H_2O_2 at applied potentials of 0.7 V, 1 V and -0.6 V vs Ag/AgCl for Ox1, Ox2 and Red, respectively. As shown, a well-defined result was obtained during the sequential increase of H_2O_2.The plots of the peak currents as a function of concentration are given in Supporting Information (SI). These findings confirm the stable and efficient catalytic property of the modified electrode. The linear range, detection of limit (DL) and sensitivity were obtained for oxidation and reduction peaks.

Figure 5

3.7. Repeatability and stability

For investigation of the repeatability of the proposed electrode, 200 µM H_2O_2 in a phosphate buffer (pH 7.0) was selected. The relative standard deviations (RSD) were calculated to be 5%, 8% and 4% for three consecutive assays of Ox1, Ox2 and Red peaks, respectively. The long term storage stability of the biosensor was tested over 28 days. When the proposed electrode was stored at laboratory temperature and measured intermittently (every 48 h), this electrode retained approximately 92%, 85% and 94% of its original response for Ox1, Ox2 and Red peaks, respectively, after 28 days of storage. The above results, therefore, indicate that this electrode has high stability and repeatability for measuring hydrogen peroxide.

3.8. Comparison of the parameters obtained for this electrode with other electrodes

The proposed electrode was compared with previous modified electrodes used for H_2O_2 measurement. The results are presented in Table 1. As can be observed, the detection of limit (DL) and dynamic range (LR) of this research are better or comparable with those of other methods for hydrogen peroxide analysis.

(Table 1)

3.9. Analytical application

In this research, various samples of milk were chosen as a real sample and the reduction peak (Red) was selected for the determination of H_2O_2 using -0.5V vs Ag/AgCl in CVs. The concentrations of H_2O_2 in two different commercial milk samples were measured using samples spiked with 50 μM and 150μM of H_2O_2 to obtain recoveries. Additionally, a blank milk sample was investigated by our method wich did not give any current response. As can be seen from Table 2, good results recoveries are obtained ranging from 97 to 102.3 %.

(Table 2)

4. Conclusion

In conclusion, a novel method for the construction of conductive DNA-based MnOx nanowire clusters by an electrochemical technique is presented. This modified electrode was based on immobilizing of DNA/MnOxNWC on a glassy carbon electrode. This electrochemical biosensor can be used for determination and detection of very low concentrations of H_2O_2 at three optional applied potentials (OX1, OX2 and Red). Electrooxidation and electro-reduction of H_2O_2 at the surface of the modified electrode was studied. The authors propose that this assembly of metal and metal oxide nanomaterials by biomolecules such as DNA will yield new hybrid nano-biomaterials with synergetic properties and functions. It is expected to be able to employ this electrochemical forming strategy to synthesize many other nanomaterials. This proposed method could be useful for future biosensor construction.

Acknowledgment

The authors gratefully acknowledge the support of this work by Iran's National Elites Foundation (INEF).

Legends to the Figures:

Schematic 1. Electrode preparation and modification.

Figure 1. **(A)** The continuous CVs for the electrodeposition of MnOx on GC/DNA electrode in 1 mM $MnSO_4.2H_2O$ and 0.1 M Na_2SO_4 in phosphate buffer solution (pH7) at scan rate of 10 mV s^{-1}. **(B)** (a) SEM image of GC/MnOx (b-c) SEM images of GC/DNA/MnOxNWC electrodes. **(C)** Cyclic voltammetry response of (a) bare (c) GC/MnOx (d) GC/DNA/MnOxNWC elctrodes in the presence of 2000 µM H_2O_2 at pH 7 and (b) GC/DNA/MnOxNWC electrode in the absence of hydrogen peroxide.

Figure 2 (**A and C)** The CVs obtained at the bare GC (a) GC/MnOx (b) GC/DNA (c) and GC/DNA/MnOxNWC (d) electrodes for the 1mM hydroquinone and 3 mM probe $[Fe(CN)_6]^{3-/4-}$ at scan rate 100 mVs^{-1}, respectively. **(B** and **D)** Electrochemical impedance spectroscopy (EIS) of (a) bare GC (b) GC/MnOx (c) GC/DNA and (d) GC/DNA/MnOxNWC electrodes in 1 mM hydroquinone and in 3 mM probe $[Fe(CN)_6]^{3-/4-}$ in the frequency range of 0.01–10^4 Hz, respectively.

Figure 3. (A) Cyclic voltammetry response of a GCE modified with DNA/MnOxNWC in a 0.10 M phosphate buffer (pH 7) containing 500 µM of hydrogen peroxide at different scan rates. **(B(a-c))** The relationship between Ip and $v^{1/2}$ and regression for (a) y =11.649x + 24.152 (R^2= 0.9964), (b) y =1.55346x + 19.276 (R^2= 0.9962) and (c) y = -74717x – 0.0338 (R^2= 0.9928).

Figure 4. (A) Cyclic voltammograms of GC/DNA/MnOxNWC electrode in buffer solution pH 7 at scan rate of 20 mVs^{-1} with increasing hydrogen peroxide concentration. **(B(a-c))** The relationship between Ip and hydrogen peroxide concentrations and regression for (a) y =0.0242x + 8.0837 (R^2= 0.9872), (b) y =0.0054x + 0.281 (R^2= 0.992) and (c) y = -0.0122x – 1.0506 (R^2= 0.9937).

Figure 5. Amperometric responses at rotating GC/DNA/MnOxNWC electrode (rotating speed 2000 rpm) in buffer solution (pH 7) at applied potentials of 0.7 V, 1 V and -0.6 V for Ox1, Ox2 and Red, respectively

Table1. Analytical parameters of several modified electrodes for determination of hydrogen peroxide.

Table 2. Determination of hydrogen peroxide content in milk samples.

References

[1] C. Shiqiang, L. Yunchun, Y. Zhousheng, W. Xianwen, Construction of silver nanowires on DNA template byan electrochemical technique, Materials and Design. 28 (2007) 722–725.

[2] J.R. Lakwicz, I. Gryczynski, Z. Gryczynski, K. Nowaczyk, C.J Murphy, Time-Resolved Spectral Observations of Cadmium-Enriched Cadmium Sulfide Nanoparticles and the Effects of DNA Oligomer Binding, Anal. Biochem. 280(2000)128–136.

[3] S Ohara, Y Hatakeyama, M Umetsu, Z Tan, T Adschiri, Fabrication of Pd–DNA and Pd–CNT hybrid nanostructures for hydrogen sensors, Advanced Powder Technology 22 (2011) 559–565

[4] N.C. Seeman, DNA nanotechnology: novel DNA constructions, Annu. Rev. Biophys. Biomol. Struct. 27(1998)225–48.

[5] S. Ensiyeh, S. Abdollah, N. Abdollah, K.A. Mohammad, Shape-dependent electron transfers kinetics and catalytic activity of NiO nanoparticles immobilized onto DNA modified electrode: fabrication of highly sensitive enzymeless glucose sensor, Biosensors and Bioelectronic.56 (2014) 313–319.

[6] E. Braun, Y. Eichen, U. Sivan, G. Ben-Yoseph, 1998. DNA-templated assembly and electrode attachment of a conducting silver wire, Nature (London).391(1998) 775-778.

[7] K. Keren, M. Krueger, R. Gilad, G. Ben-Yoseph, U. Sivan, E. Braun, Sequence-specific molecular lithography on single DNA molecules, Science (Washington, D.C.). 297(2002) 72-75.

[8] R. Seidel, M. Mertig, W. Pompe, Scanning force microscopy of DNA metallization, Surf. Interface Anal. 33(2002)151-154.

[9] J. Richter, R. Seidel, R. Kirsch, M. Mertig, W. Pompe, J. Plaschke, H.K. Schackert, Nanoscale Palladium Metallization of DNA, AdV. Mater. 12(2000)507-510.

[10] Z. Keying, Z. Na, W. Cong, G. Tao, Amperometric sensing of hydrogen peroxide using a glassy cabon electode modified with silver nanoparticles on poly (alizarin yellow R), Microchim. Acta. 173(2011)135–141.

[11] M.S.M. Quintino, H. Winnischofer, K. Toma, L. Angnes, Cobalt oxide/tetraruthenated cobalt-porphyrin composite for hydrogen peroxide amperometric sensors, Analyst .130(2005) 221-26.

[12] N.V. Klassen, D. Marchington, H.C.E. Mcgowan, H_2O_2 determination by the I3- method and by $KMnO_4$ titration, Anal. Chem. 66 (1994) 2921-25.

[13] P.A. Tanner, A.Y.S. Wong, Spectrophotometric determination of hydrogen peroxide in rainwater, Anal. Chim. Acta. 370 (1998)279-87.

[14] T. Taniai, A. Sakuragawa, T. Okutani, Fluorometric Determination of Hydrogen Peroxide in Natural Water Samples by Flow Injection Analysis with a Reaction Column of Peroxidase Immobilized onto Chitosan Beads, Anal. Sci. 15(1999) 1077-82.

[15] J.C. Yuan, A.M, Shiller. Anal. Chem., Determination of Subnanomolar Levels of Hydrogen Peroxide in Seawater by Reagent-Injection Chemiluminescence Detection, Analytical Chemistry. 71(1999) 1975-80.

[16] S. Effkemann, U. Pinkernell, U. Karst, Peroxide analysis in laundry detergents using liquid chromatography, Anal. Chim. Acta. 363(1998) 97-103.

[17] T. Soundappan, W. Buo, C. Shen-Ming, Nano TiO_2–Au–KI film sensor for the electrocatalytic oxidation of hydrogen peroxide, Sensors and Actuators B. 136(2009)464-471.

[18] S. Mojtaba, Mehdi, A, G. Mohammad, A novel impedimetric nanobiosensor for low level determination of hydrogen peroxide based on biocatalysis of catalase, Bioelectrochemistry. 83(2012) 31–37.

[19] J. Feng, J.J Xu, H.Y Chen, Direct electron transfer and electrocatalysis of hemoglobin adsorbed on mesoporous carbon through layer-by-layer assembly, Biosens Bioelectron. 22(2007)1618-1624.

[20] Y. Hasebe, T. Gu, DNA–Cu(II) complex as a novel electrocatalyst for a hydrogen peroxide sensor, J Electroanal Chem. 576(2005)177-81.

[21] J. Shobha, S. Ramaprabhu, N.S. Sriman, A thionine functionalized multiwalled carbon nanotube modified electrode for the determination of hydrogen peroxide, Carbon. 45(2007) 1340-53.

[22] B. Zhao, Z.R. Liu, Z.L. Liu, G.X. Liu, Z. Li, J.X. Wang, X.T. Dong, Silver microspheres for application as hydrogen peroxide sensor, Electrochem Commun. 11(2009)1707-10.

[23] M.R. Mahmoudian, Y. Aliasa, W.J. Basirun, M.W.M. Pei, Facile preparation of MnO_2 nanotubes/reduced graphene oxide nanocomposite for electrochemical sensing of hydrogen peroxide, Sensors and Actuators B. 201 (2014) 526–534.

[24] E. Turkusica, J. Kalcher, E. Kahrovi, N.W. Beyene, H. Moderegger, E. Sofic, S. Begic, K. Kalcher, Amperometric determination of bonded glucose with an MnO_2 and glucose oxidase bulk-modified screen-printed electrode using flow-injection analysis, Talanta, 65(2005) 559-564.

[25] S.W. Donne, G.A. Lawrence, A.J. Swinkels, The chemostat: A novel approach to the synthesis of manganese dioxide, Mater. Res.Bull. 30(1995) 859-69.

[26] X.L. Luo, J.J. Xu, W. Zhao, H.Y. Chen, A novel glucose ENFET based on the special reactivity of MnO2 nanoparticles, Biosens. Bioelectron. 19(2004)1295-300.

[27] S.C. Pang, M.A. Anderson, T.W.J. Chapman, Novel Electrode Materials for Thin- Film Ultracapacitors: Comparison of Electrochemical Properties of Sol- Gel- Derived and Electrodeposited Manganese Dioxide, Electrochem.Soc. 147(2000) 444-50.

[28] F.L. Cras, S. Rohs, M. Anne, P.J. Strobel, Reversibility of lithium intercalation in lithium and sodium phyllomanganates, Power Sources.54(1995) 319-322.

[29] F. Pagnanelli, C. Sambenedetto, G. Furlani, F. Vegliò, L. J Toro, Preparation and characterisation of chemical manganese dioxide: Effect of the operating conditions,Power Sources. 166(2007)567-77.

[30] M.Q. Wu, G.A. Snook, G.Z. Chen, D.J. Fray, Redox deposition of manganese oxide on graphite for supercapacitors, Electrochem.Commun. 6(2004) 499-504.

[31] T. Shinomiya, V. Gupta, N. Miura, Effects of electrochemical-deposition method and microstructure on the capacitive characteristics of nano-sized manganese oxide , Electrochim. Acta.51(2006) 4412-19.

[32] J.P. Petitpierre, C. Comninellis, E. Plattner, Oxydation Du MnSO4 en dioxyde de manganese dans H_2SO_4 30%, Electrochimica Acta. 35(1990) 281-87.

[33] Z. Rogulski, H. Siwek, I. Paleska, A. Czerwinski, Electrochemical behavior of manganese dioxide on a gold electrode, Journal of Electroanalytical Chemistry.543(2003) 175-85.

[34] A.J. Bard, 1973. Encyclopedia of Electrochemistry of the Elements, vol. 1, MarcelDekker, New York.

[35] B.L. Wu, D. Lincot, J. Vedel L.T. Yu, Voltammetric and electrogravimetric study of manganese dioxide thin film electrodes. Part 1. Electrodeposited films, Journal of Electroanalytical Chemistry. 420(1997) 159-165.

[36] M.M. Samira, T. Hazhir. S. Abdollah H. Rahman. Fabrication of electrochemical theophylline sensor based on manganese oxide nanoparticles/ionic liquid/chitosan nanocomposite modified glassy carbon electrode, Electrochimica Acta. 108(2013) 707–716.

[37] B.G. Mohammad, S. Mojtaba, A. Nader, Nonenzymatic L-lysine amino acid detection using titanium oxide nanoparticles/multi wall carbon nanotube composite electrodes, Electrochimica Acta. 123(2014)569–575.

[38] P.M.U. Anu, V. Anuraj, B. Satpati, R. Srivastav. Facile preparation of Ni(OH)2–MnO2 hybrid material and its application in the electrocatalytic oxidation of hydrazine, Journal of Hazardous Materials. 262(2013) 766– 774.

[39] L. Hongying, G. Chunchuan. L.Dujuan, Z. Mingzhen, Non-enzymatic hydrogen peroxide biosensor based on rose-shaped FeMoO4 nanostructures produced by convenient microwave-hydrothermal method, Materials Research Bulletin.64(2015) 375-379.

[40] N. Yongnian, K. Serge, A novel electrochemical sensor based on the copper-doped copper oxide nano-particles for the analysis of hydrogen peroxide, Colloids and Surfaces A: Physicochem. Eng. Aspects. 465(2015) 153–158.

[41] C. Erhan, S. Berika, A. Müge, E. Kıran, MWCNT–cysteamine–Nafion modified gold electrode based on myoglobin for determination of hydrogen peroxide and nitrite, Bioelectrochemistry. 101(2015)126–131.

[42] A.G. Vasiliki, A. G.,L.G. Dimothenis, G.V.Athanasios, I.P. Mamas , Rhodium nanoparticle-modified screen-printed graphite electrodes for the determination of hydrogen peroxide in tea extracts in the presence of oxygen, Talanta. 134(2015) 482‑87.

[43] Q.Xia, W. Huicai, M. Zhiying, L. Junli, C. Qiang, A novel non-enzyme hydrogen peroxide sensor based on catalytic reduction property of silver nanowires,Talanta. 139(2015) 56‑61.

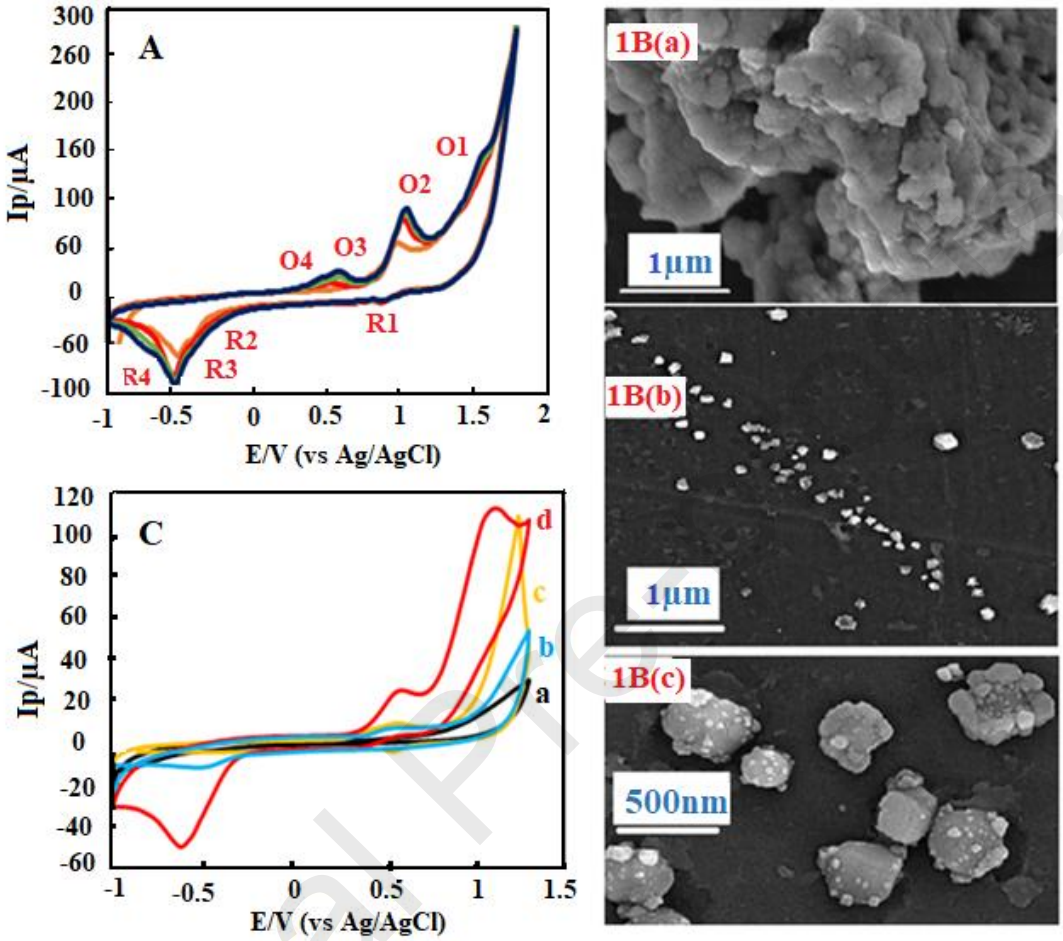
A
Ip/μA
E/V (vs Ag/AgCl)
O1
O2
O3
O4
R1
R2
R3
R4
C
d
c
b
a
1B(a)
1μm
1B(b)
1μm
1B(c)
500nm

Fig.1

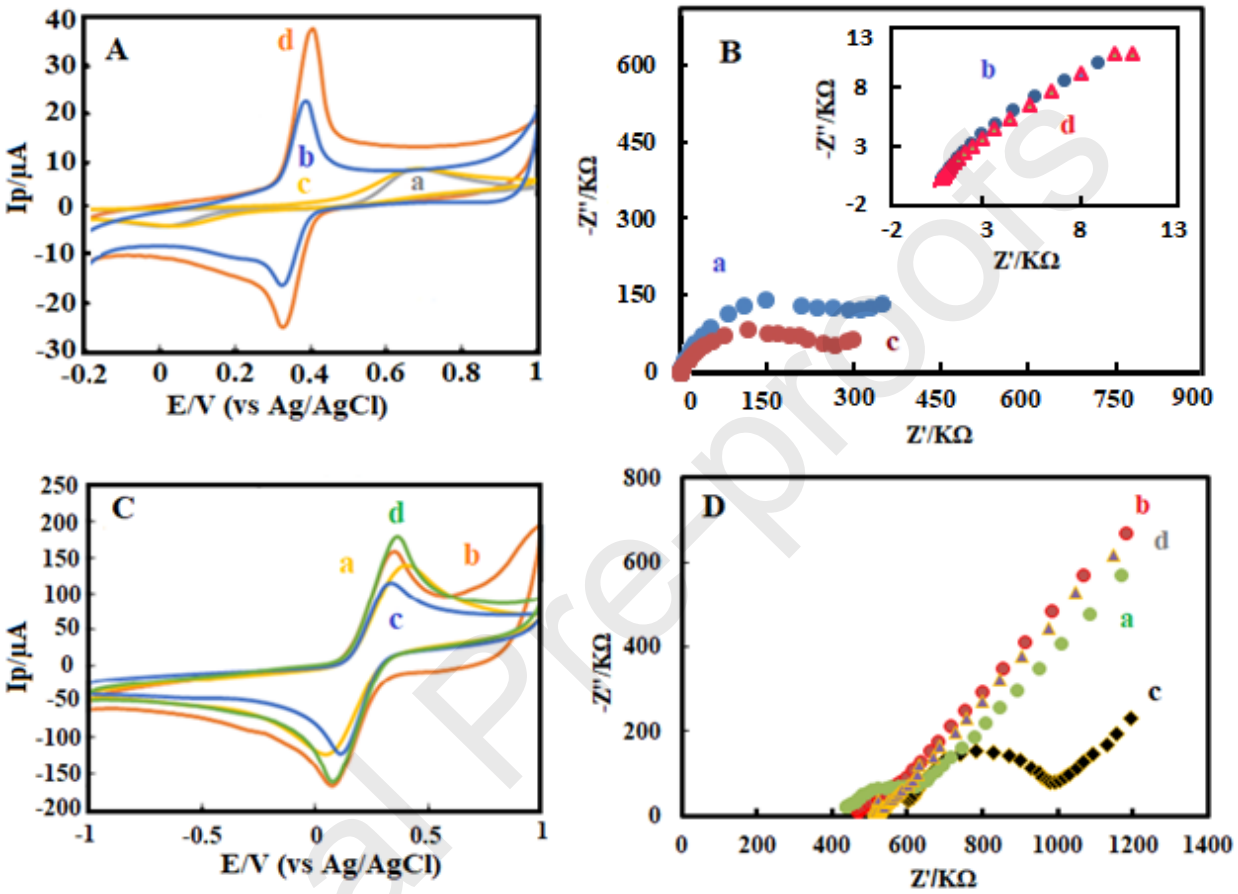

Fig.2

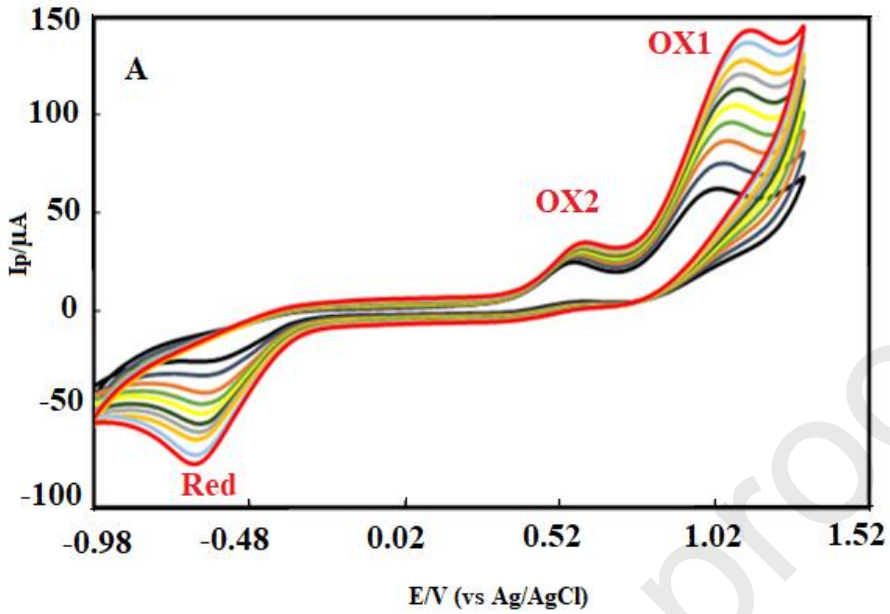

Fig. 3A

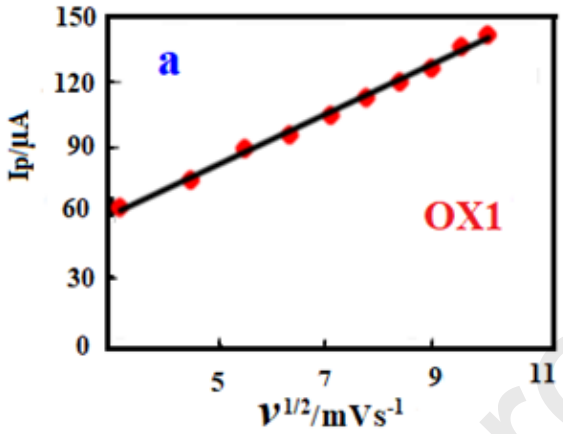

Fig.3B(a)

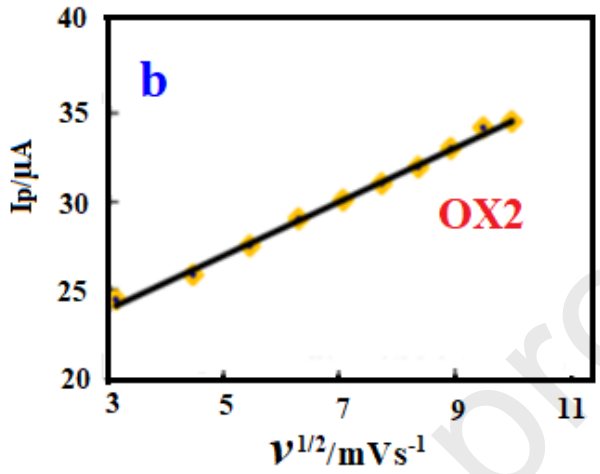

Fig.3B(b)

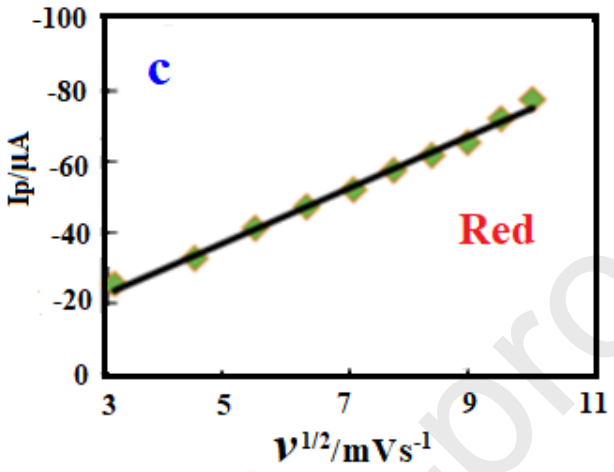

Fig.3B(c)

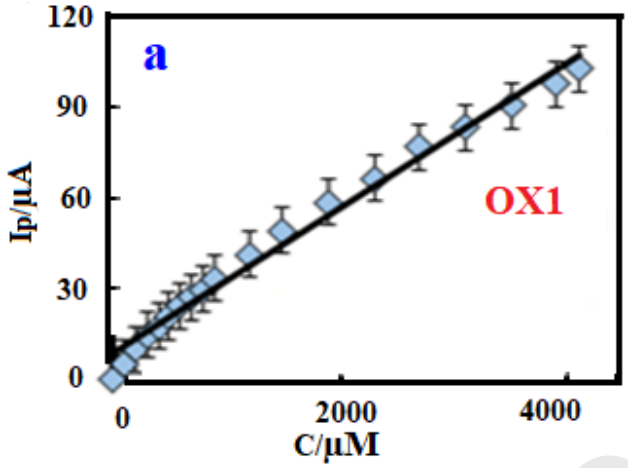

Fig.4B(a)

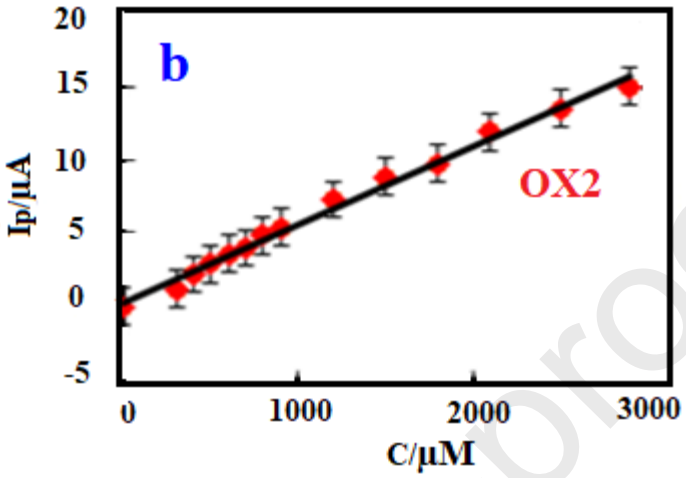

Fig.4B(b)

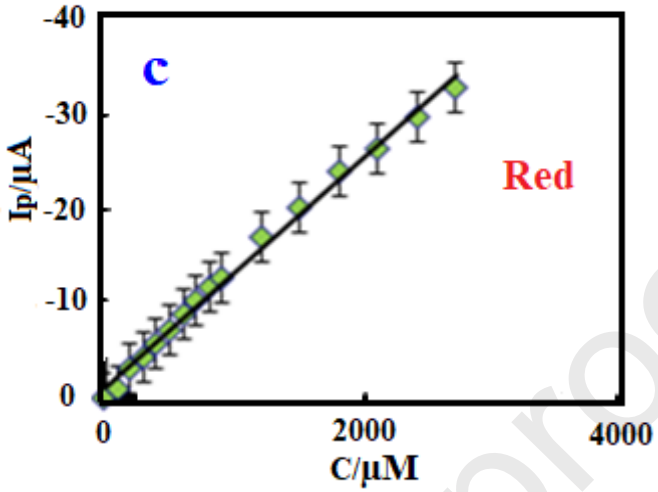

Fig.4B(c)

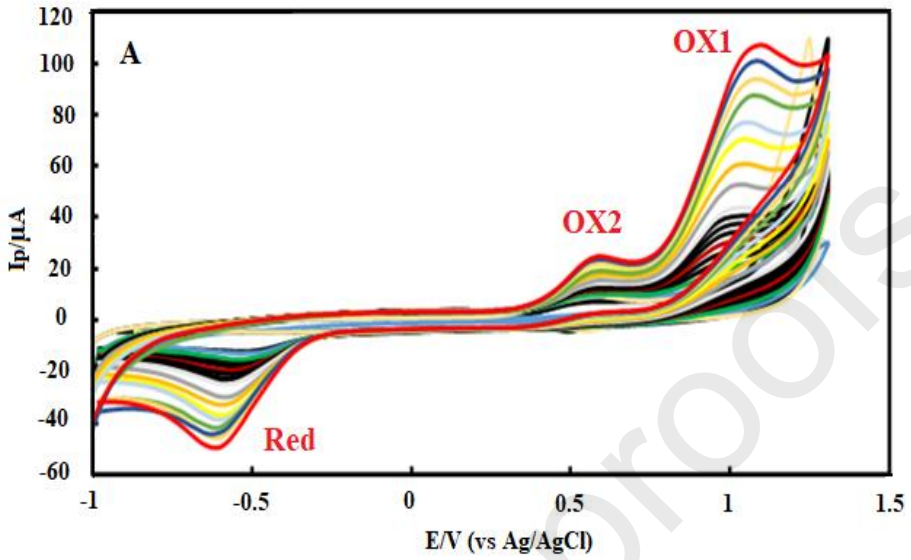

Fig.4A

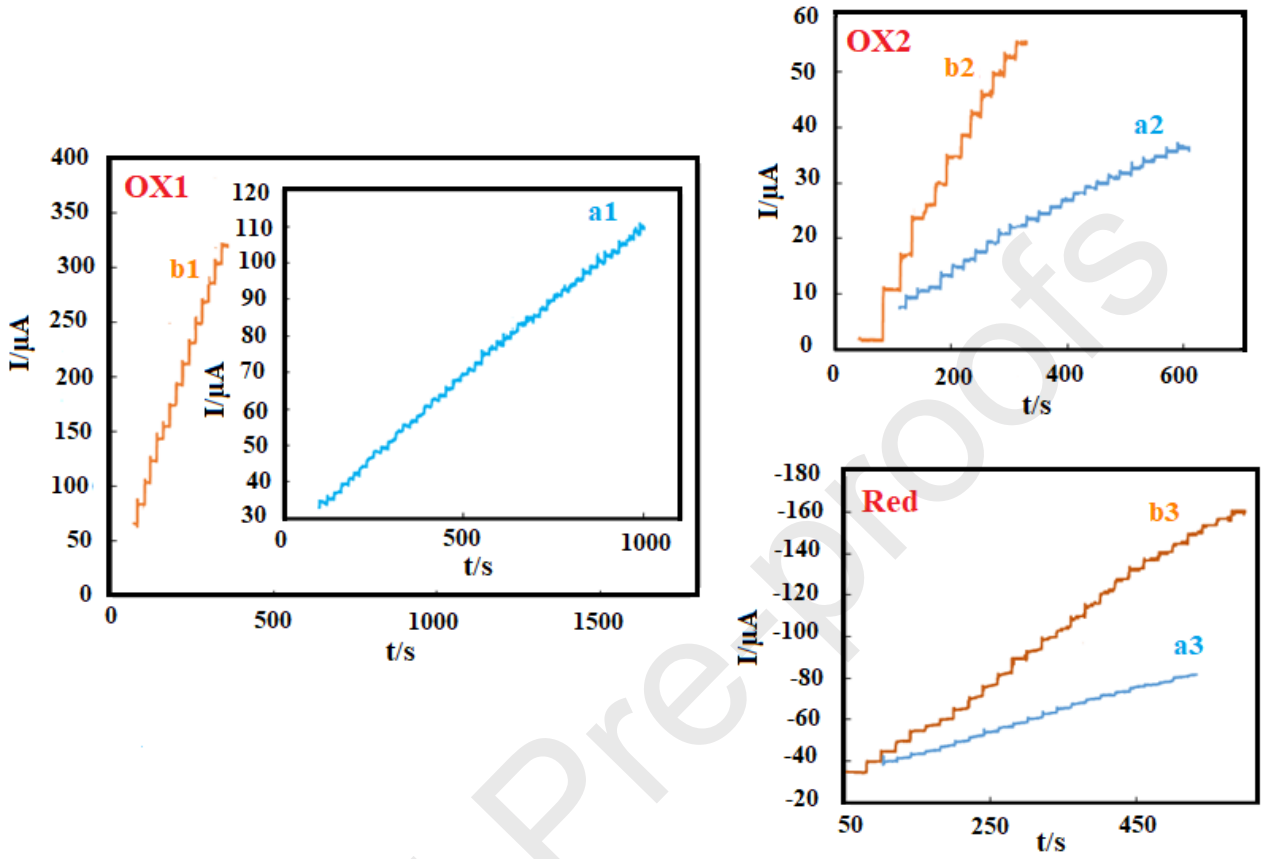

Fig.5

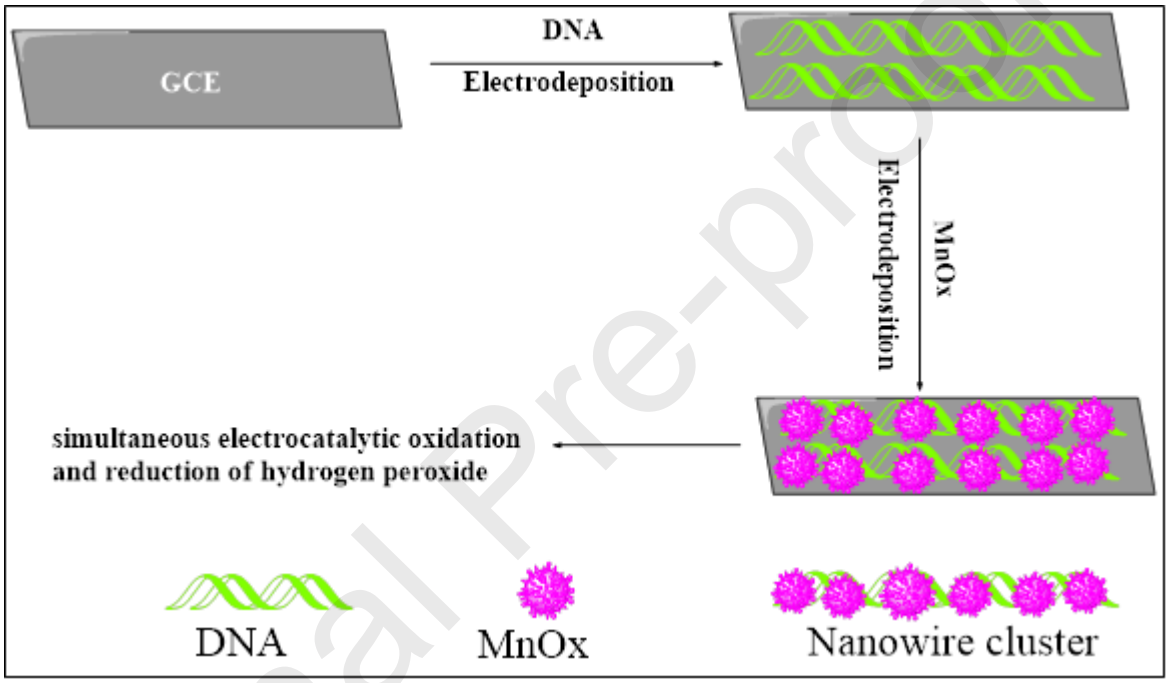

Schematic 1

Table 1. Analytical parameters of several modified electrodes for determination of H_2O_2

Electrode	sensivity	LOD	Dynamic rang	Ref
$FeMoO_4$	-	0.5mM	1-1.6mM	[39]
Cu doped Copperoxide NPs	-	0.23mM M	0.005-8mM	[40]
MWCNT/Cystamine/Nafion	-	0.0 1µM	0.1-70 µM	[41]
Rd NPs/Graphite	-	2 µM	5-600 µM	[42]
Silver NPs	9.45µA/mM	0.2 µM	0.5µM-30mM	[43]
Ox1	328mA/mM	1.1 µM	5 µM-1.4mM	This work
Ox2	240mA/mM	2.9 µM	5 µM-1.3mM	This work
Red	412mA/mM	1.3 µM	5 µM-2.7mM	This work

Table 2. Determination of H_2O_2 in milk samples

Sample	Added (μM)	Found (μM)	Recovery (%)
1	50	59	100.8
	150	152	101.3
2	50	48.5	97
	150	153.3	102.3

Graphical abstract

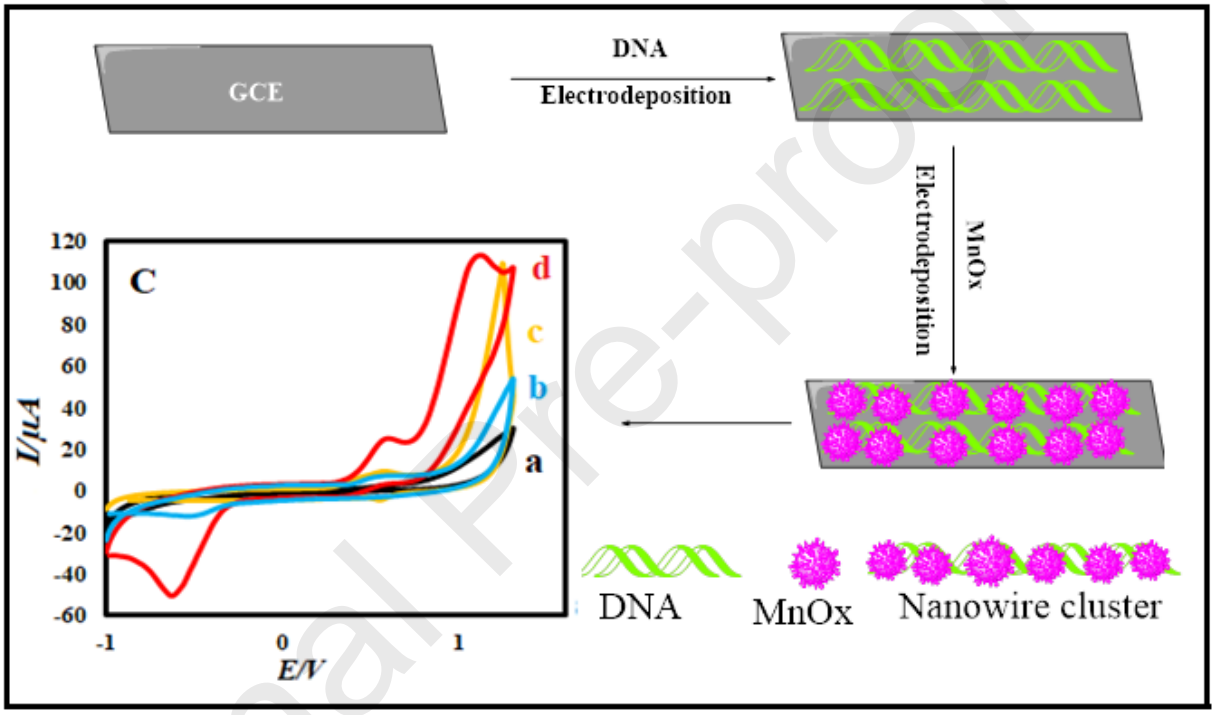

Highlights

►MnOx nanowire-like clusters prepared using DNA as template ► Electrocatalytic oxidation and reduction of H_2O_2 at three applied potentials► Mechanisms proposed for MnOx nanowire-like cluster ► Mechanisms proposed for oxidation and reduction of H_2O_2